Renewable and Sustainable Energy Reviews 15 (2011) 612–620

Contents lists available at ScienceDirect

Renewable and Sustainable Energy Reviews

journal homepage: www.elsevier.com/locate/rser

An offshore wind atlas for the Canary Islands

A.C. Martín Mederos [a], J.F. Medina Padrón [b], A.E. Feijóo Lorenzo [c,*]

[a] Zona Eólica Canaria S.A., Veintinueve de Abril, 30, Las Palmas 35007, Spain
[b] Departamento de Ingeniería Eléctrica, Universidad de Las Palmas de Gran Canaria, 35017 Las Palmas, Spain
[c] Departamento de Enxeñería Eléctrica, Universidade de Vigo, ETSEI, Campus de Lagoas-Marcosende, 36310 Vigo, Spain

ARTICLE INFO

Article history:
Received 30 July 2010
Accepted 3 August 2010

Keywords:
Offshore wind farms
Wind energy

ABSTRACT

In this paper an analysis of the offshore wind potential in the Canary Islands is presented in the shape of a set of wind maps which constitute an offshore wind atlas. It has been drawn up using data processed from 40 weather stations and satellite. Results from satellite mapping, limited area modelling and mesoscalar modelling have been used by applying the technique known as 'one way nesting'.

Contents

1. Introduction

A wind atlas is an important tool for optimal exploitation of wind resources [1,2]. The offshore wind atlas of the Canary Islands [3,4] is a geographic chart that gives information about three important wind features: mean wind speed, wind direction and wind potential at different locations around the islands. In the following sections an explanation has been included of the steps that have been followed to compile data and establish the charts for this atlas, and graphs are given to reveal the results obtained.

2. Stages of the work

The atlas has been developed in the following six stages:

1. Definition of the research area.

* Corresponding author.
E-mail addresses: gerente@zecsa.org (A.C. Martín Mederos), jmedina@die.ulpgc.es (J.F. Medina Padrón), afeijoo@uvigo.es (A.E. Feijóo Lorenzo).

1364-0321/$ – see front matter
doi:10.1016/j.rser.2010.08.005

2. Data collection from different anemometer stations.
3. Obtaining of maps from numerical models and satellites.
4. Statistical data processing.
5. Calculation and elaboration of the offshore wind atlas.
6. Data extrapolation.

In the following sections the six previous steps are explained in detail.

3. Definition of the research area

The first step for the elaboration of a wind atlas (regardless of whether it is offshore, inshore or nearshore) consists of defining the working area limits, which constitute what has been denoted as working domain in this work. In this case the limits of the geographic area are given by the parallels of northern latitude 29 ° 55′00″ and 26 ° 41′00″, and the meridians of western longitude 18 ° 50′00″ and 12 ° 38′00″.

This means the studied area comes to 212,760 km^2, and contains the 7 main islands, i.e., El Hierro, La Palma, La Gomera, Tenerife, Gran Canaria, Fuerteventura and Lanzarote, and the 6 smaller islands, i.e., Alegranza, La Graciosa, Montaña Clara, Lobos, Roque del Este, Roque del Oeste, together with a small part of the African coast, belonging to Western Sahara [5,6]. Geographic information handled in this work has been given by SITCAN, which is the *Sistema de Información Territorial de Canarias* (Territorial Information System of the Canary Islands).

4. Data collection from different anemometer stations

Anemometer stations for data collection must be sought according to the following criteria:

1. These stations have to measure the sought after data, of course, such as wind speed and direction in this case.
2. It is important to have data for 3 years, at least.
3. They should be located as close as possible to the area being studied.
4. They have to be rigorously controlled when acquiring, storing, correcting and verifying data.

Data from 40 weather stations have been handled for the elaboration of this atlas. Their locations on the different islands are the following: 2 stations are on El Hierro, 2 on La Palma, 2 on La Gomera, 15 on Tenerife, 11 on Gran Canaria, 3 on Fuerteventura and 3 on Lanzarote. 2 stations are buoys floating in the Atlantic Ocean, one of them to the south of the island of Tenerife and the other one at the northwest of Gran Canaria. So, the quantity of acquired data comes to 2,102,400, i.e., 2 data (wind speed and direction) per hour during 3 years (24×365 hours per year) for the 40 stations.

5. Obtaining of maps from numerical models and satellites

Comparative studies have shown that correct simulation of a phenomenon depends on the specific configuration and options used for its modelling. It is not so important to work with a given numerical model for weather prediction, but rather to choose an adequate parametrization and configuration [7]. A bibliography review has been made into different modelling configurations, interaction techniques, resolution, and model application [8–11]. Configurations of operational models in several meteorological institutions have been studied, and also some research works where meteorological models have been applied to the analysis of weather phenomena.

The final conclusion has been that a good solution is to apply a technique known as 'one way nesting', that is to say, interaction in one direction [12]. This technique groups together results obtained from:

1. Satellite mapping (QuickSCAT).
2. Limited area modelling (HIRLAM).
3. Mesoscalar modelling (MM5).

Another requirement for this work is to have very powerful hardware for calculations. This can be substituted by requesting data from those international institutions that are able to provide them.

As for satellite mapping we should comment that data have been provided by the NASA (US National Aeronautics and Space Administration) QuickSCAT satellite [13,14], which contains a microwave radar sensor that can measure reflexion or dispersion produced as it explores the Earth's surface. This radar was specifically developed for measuring wind speed and direction near the ocean surface and has three subsystems: SES (electronic subsystem), SAS (antenna subsystem), and CDES (command and data subsystem).

The SES is the core of the module and contains a transmitter, a receiver and a processor for numerical signals. It generates and sends radiofrequency waves to the SAS, which sends the signal to the Earth by means of pulses. These pulses reach the ocean surface and experience an echo effect, known as backscatter. This backscatter is redirected by the SAS to the SES, and this system converts the received signal to facilitate its processing. The CDES is basically a computer with the software needed to operate the whole system correctly. One of the operations the CDES has to carry out is to calculate, with minimum error, the position of the signal on the Earth's surface. The CDES also stores the temperature of the system and operating currents and voltages to supervise the state of the device.

Data given by this satellite are particularly important for drawing up the offshore wind atlas as they allow us to know not only the interaction between earth and ocean but also about ocean streams, together with their effects on global climate behavior.

In Fig. 1 an example is shown of a map of ocean winds at a height of 10 m. Data have been processed by NOAA/NESDIS (National Oceanic and Atmospheric Administration/National Environmental Satellite Data and Information Service) [15], from data obtained by NASA/JPL (Jet Propulsion Laboratory), by means of QuicSCAT. These images have a resolution of 20 km and have been adapted to a grid made specifically for the Canary Islands offshore wind atlas. This grid contains 31 columns and 21 rows, which results in 651 smaller rectangles, not all of them completed.

The fact that images are captured once per day should been taken into account. Data corresponding to 4 years have been requested (period 2003–2006), which means a total of 1,900,920 data. The mean value for every rectangle is calculated from all these data.

By applying a 'one way nesting' technique, these data will serve as a reference for correcting the HIRLAM model [16,17]. The goal of the correction is to avoid excessive deviations in the final results, and consists of establishing maximum and minimum values at 115% and 85% of the calculated mean value. So, values outside these limits are corrected and restricted to them.

The HIRLAM model, in operation in the Spanish Weather Agency AEMET (formerly known as INM), has the following main features:

1. Two possible horizontal resolutions: 0.16 ° and 0.05 °.
2. Vertical resolution: 40 hybrid levels.

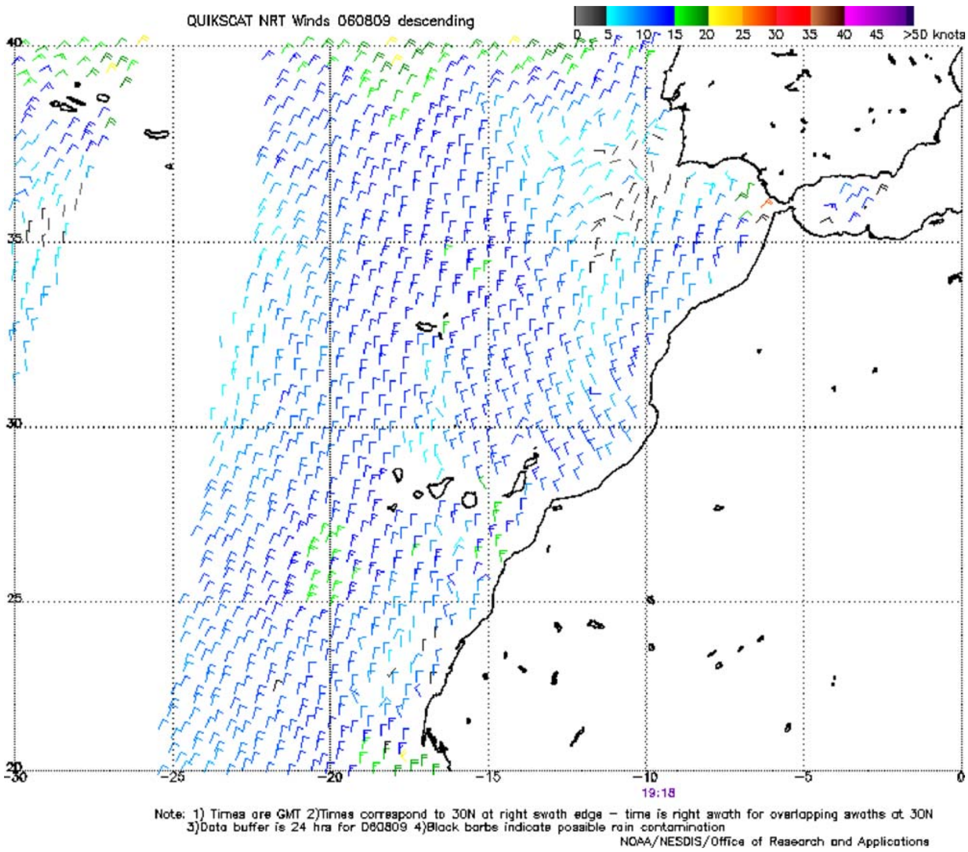


Fig. 1. Wind speed and wind direction obtained from the QuickSCAT satellite.

3. Mesh resolution: 9 km.
4. First guess: predictions based on registers taken 6 h before with the same model.
5. Analysis:
(a) Height:
i. Data assimilation: intermittent every 6 h with a data window of −3 to +2 h.
ii. Variables: temperature, wind, relative humidity.
iii. Method: three-dimensional variational.
(b) Surface:
i. Variables: ocean water temperature, pressure at ocean level, wind speed at 10 m altitude and temperature at 2 m.
ii. Method: univariant.
6. Initialization: by digital filtering.
7. Prediction:
(a) Dependent variables: pressure at surface level, temperature, wind and specific humidity.
(b) Vertical representation: finite differences, energy conservation, angular moment.
(c) Horizontal representation: finite differences, Arakawa C grid.
(d) Integration time: Leapfrog, semi-implicit with time step equal to 2 or 4 min.
(e) Horizontal diffusion: implicit 4th order.
(f) Vertical diffusion: limit layer.
(g) Dynamic: Semilagrangian.

An image extracted from the map generated by the AEMET is shown in Fig. 2.

From maps received from AEMET [18], a mesh has been built with a resolution of 9 km, consisting of 66 rectangles in west-east direction (horizontal), and 40 rectangles in north-south direction (vertical), which gives 2640 computable rectangles.

It has been applied in the running of the HIRLAM model for the 5-year period 2002–2006. This model presents data for 4 daily passings (at 00:00, 06:00, 12:00 and 18:00). By calculating the total number of data on the basis of the product explained earlier, the number of total data handled is 38,544,000, where wind speed and direction are included. The mean values are obtained to calculate one rectangle.

Similar to what happens with satellite images, the technique of interaction in one direction is employed, such that the data of the 9 km domain will serve as reference for the correction of the MM5 model [19]. Such a correction consists of restricting values above 115% or below 85% of the value calculated by HIRLAM, as mentioned before.

Focusing on the MM5 model, whose data are obtained by the ITER (*Instituto Tecnológico de Energías Renovables*) [20] and the RIU

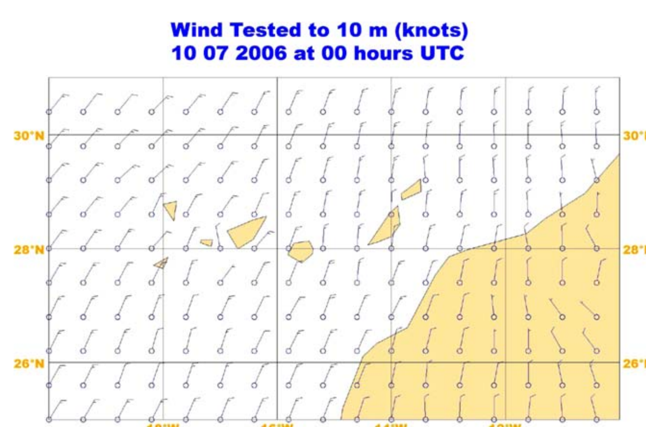


Fig. 2. Image by HIRLAM model extracted from AEMET.

(*Red Ibérica de Usuarios de MM5*) [21], the most relevant aspects of the version used (3.6) are the following:

- Capacity for multiple nesting in both directions between domains, which facilitates the analysis of atmospheric phenomena for different time scales, and the design of very high resolution predictions.
- Formulation of a non-hydrostatic dynamic, which allows the effective use of the model to represent phenomena of very small size in km.
- Data adaptation for using on multiple platforms and multitasking execution in parallel computing.
- Automatic initialization with different sources of meteorological analysis and observations, including the ability to assimilate four-dimensional data.
- Introduction of the most modern and realistic parametrization schemes for physical processes with regard to atmospheric radiation, micro-physics of clouds and precipitations, cumulus convection, turbulence and energy flows and moment over the Earth's surface.

The data for initializing the model come from the global model GFS (Global Forecast System) [22,23] for the initial contour conditions. A relatively high horizontal resolution was chosen for MM5 to be able to show meteorological phenomena that affect the islands with enough detail.

As a test of the results given by MM5 model, an assessment has been made for some days with a modern model, WRF (Weather Research and Forecasting model) [24], and the conclusion was that the results were almost identical.

The numerical values of wind speed and direction given by MM5 belong to the period 2004–2006, with a resolution of 3 km, which involves a mesh of 197 rectangles in west–east direction and 120 in north–south direction. This means 23,640 rectangles.

The MM5 model uses data from 8 daily passings (at 00:00, 03:00, 06:00, 09:00, 12:00, 15:00, 18:00 and 21:00). Multiplying the number of rectangles by the number of years, the days per year, the number of passings and 2 (because there are two variables, speed and direction), a total amount of 414,172,800 data are obtained. The mean value is what is taken into account.

As a summary, the total number of data used with the three models is 454,617,720. Due to this, a data sheet has been used for each model and year, using Open Office Calc. The results of the maps are refreshed automatically when there are new data.

6. Statistical data processing

Due to the large amount of data to be processed, that is to say, 454,617,720 from the prediction models, and 2,102,400 from the anemometer measurements, a very exhaustive control of data collection is required.

6.1. Prediction model data analysis

Once these data have been introduced in the different data sheets, an algorithm has to be run to search for values greater than 35 m/s or lower than 0 m/s, and erroneous values. In this last case they are substituted by assumed valid values by means of an interpolation of the nearest values in the data register.

Data from the different prediction models are compared with those of the verifying equation in order to check if they are identical.

6.2. Anemometer station measurements test

Wind speed data have been taken from anemometer stations existing inside the working domain. Each station provides the wind speed in m/s and wind direction at a given altitude Z_g. The reference for wind direction is the east direction. North direction means 90 ° and so on.

So, data from anemometer stations and those from prediction models are given in the same reference frame and measurement units, in the International System.

7. Calculation and elaboration of the offshore wind atlas

The offshore wind atlas for the Canary Islands has been defined on the basis of mean wind speed and mean direction at 10 m height. The values employed are the result of the interaction between three domains of the three prediction models (satellite mapping, HIRLAM model and MM5 one). The results are given for a resolution of 3 km. These values are corrected with data from the anemometer stations. The coastal data for the islands are the result of an interpolation between the values of prediction models with a weight of 65%, and the value taken at the nearest anemometer, with a weight of 35%. At 6 km of the coast this correction is negligible.

7.1. Mean wind speed

Mean wind speeds at a height of 10 m can be seen in Fig. 3. This map shows interesting information about the best locations according to wind speed. The areas with best features seem to be the south and southeast part of the island of Gran Canaria, the area between Tenerife and west–northwest of Gran Canaria, southeast of the island of El Hierro, northeast of La Palma, and northwest of La Gomera. In all these locations mean wind speeds can reach values in the interval of 8–10 m/s.

In the case of Lanzarote and Fuerteventura the mean wind speeds are in the interval of 4–6 m/s, and the worst areas from the point of view of wind speed are located in the southwest of Tenerife and La Palma, with values between 3 and 4 m/s.

7.2. Wind direction

On the other hand the mean wind direction maps can be seen in Figs. 4–6.

According to the 8 main directions and to the reference explained (0 ° for east direction), the following notation has been included in the maps:

- East: from 337.5 ° to 22.5 °, symbol→.
- Northeast: from 22.5 ° to 67.5 °, symbol ↗.
- North: from 67.5 ° to 112.5 °, symbol ↑.
- Northwest: from 112.5 ° to 157.5 °, symbol ↖.
- West: from 157.5 ° to 202.5 °, symbol ←.
- Southwest: from 202.5 ° to 247.5 °, symbol ↙.
- South: from 247.5 ° to 292.5 °, symbol ↓.
- Southeast: from 292.5 ° to 337.5 °, symbol ↘.

By looking at the maps we can say that the wind comes mainly from the north, although there are certain areas where other directions dominate, such as northwest, northeast or east.

Although the mean value has been represented on the maps, an interesting subject is to check if this value is actually representative, for which two statistical values have been calculated:

The first one is a measurement of dispersion, and is given by the standard deviation, defined in (1):

$$S = \sqrt{\frac{\sum_{i=1}^{n}(x_i - \bar{X})^2}{n}} \tag{1}$$

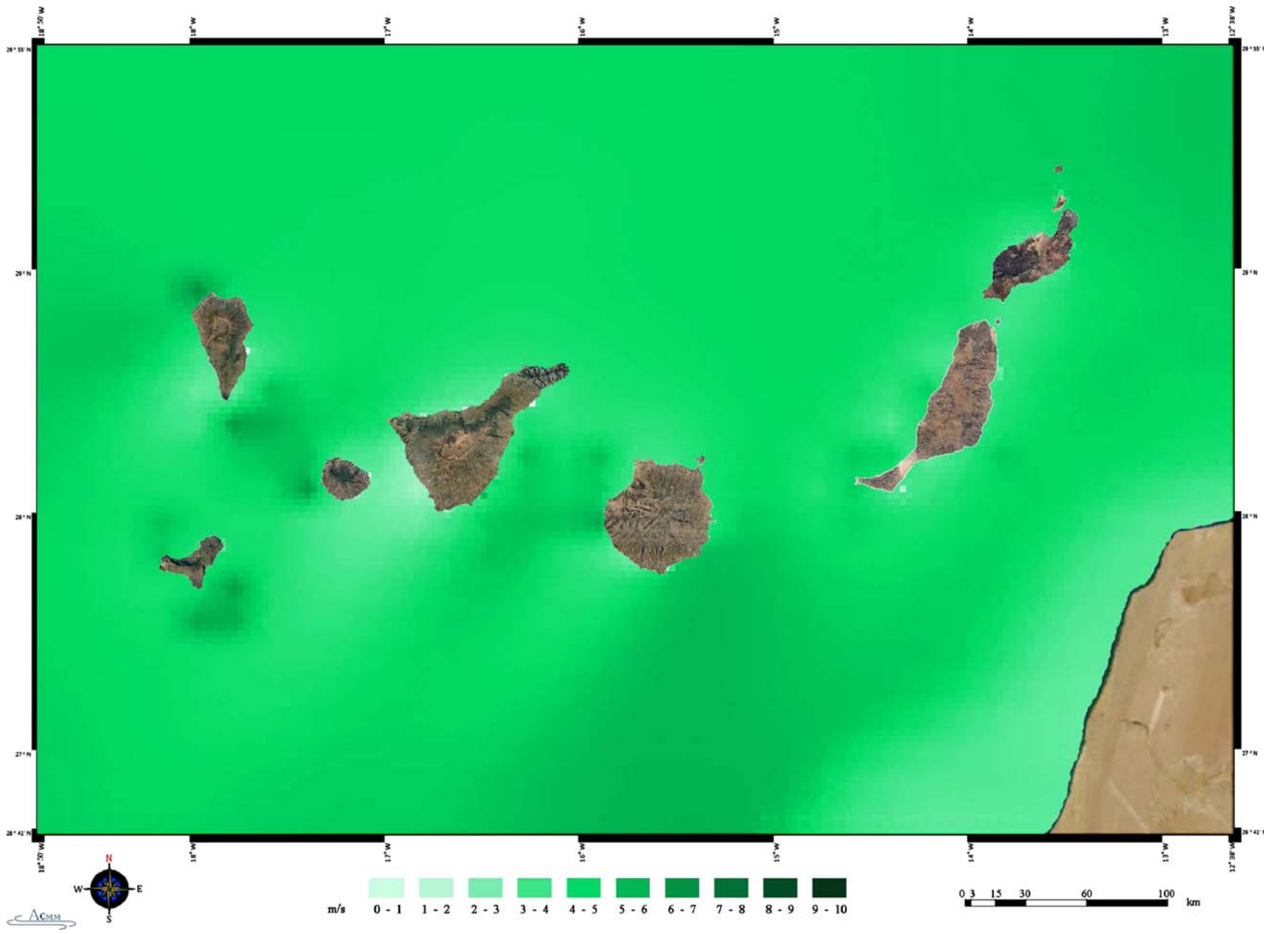


Fig. 3. Mean wind speed.

where:

- x_i is a given speed or direction value.
- n is the number of speed or direction samples.
- $\bar{X}$ is the mean speed or mean direction value, which is calculated as $\bar{X} = \sum_{i=1}^{n} x_i/n$.

The mean wind speed seems to be a more reliable value than the direction, because its standard deviation always remains at values in the interval of 3–4 m/s, whereas the standard deviation for direction reaches values of 100 °.

There is also a measurement of shape and concentration, given by the Fisher asymmetry coefficient (2):

$$\gamma = \frac{\sum_{i=1}^{n} (x_i - \bar{X})^3 \cdot f_i}{S^3} \tag{2}$$

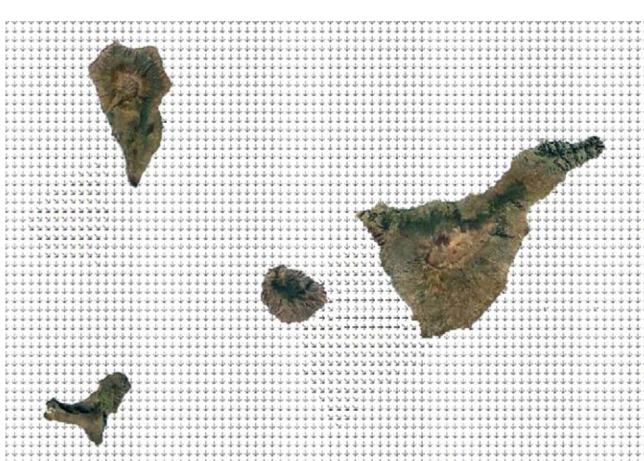


Fig. 4. Mean wind direction – western area.

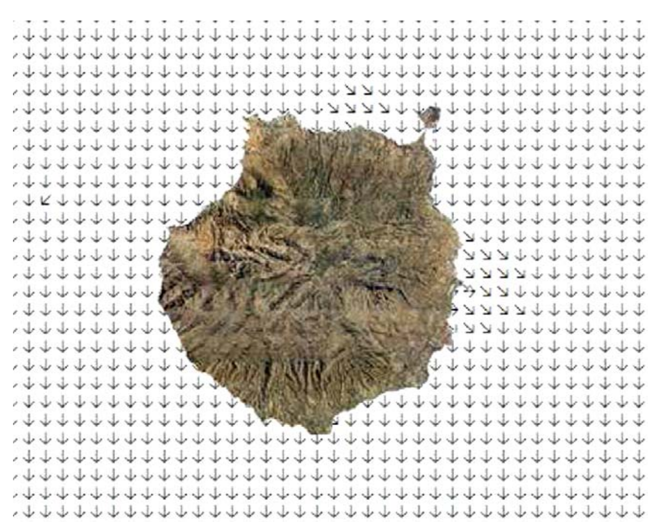


Fig. 5. Mean wind direction – middle area.

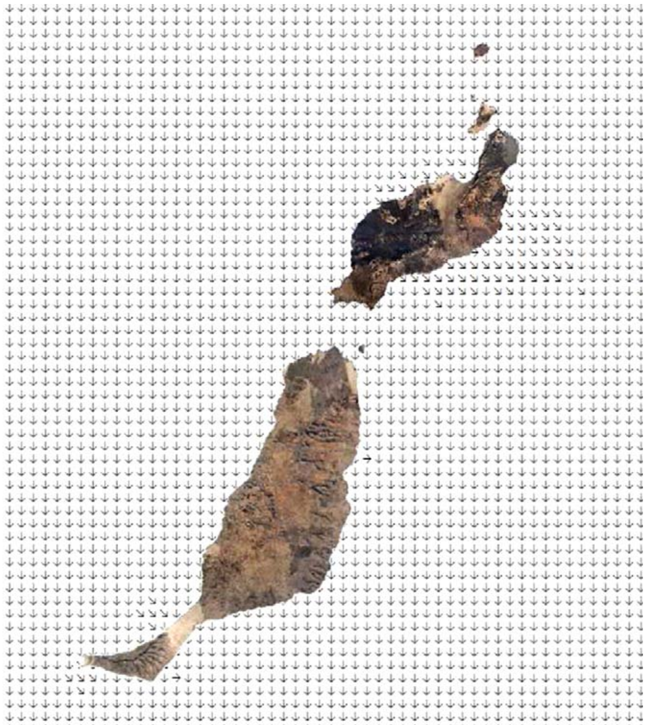


Fig. 6. Mean wind direction – eastern area.

where:

- x_i, n, $\bar{X}$ and S mean the same as in (1).
- f_i is the frequency of each value.

According to this coefficient, the distribution can be considered symmetrical if $\gamma = 0$. It can be said that both mean speeds and directions tend to a symmetrical distribution, although in the case of mean speeds, values close to 2 or -2 are also reached.

A new and different set of three maps have been drawn up and represented in Figs. 7–9, where the dominant direction of the wind has been represented.

The conclusion is that the northeast direction is dominant for 85% of the domains, although north and northwest are also dominant directions in some cases.

The assumption has been made that there is no need to estimate mean directions and mean speeds over a long term period by means of methods such as Corotis [25] or Box-Jenkins [26]. This is because the fact has been assumed that, in the least favorable situation, a series of 3 years measurements is available for study. According to research works by Corotis, this means that there is a 90% confidence level for the mean value of direction or speed over the next 20 years.

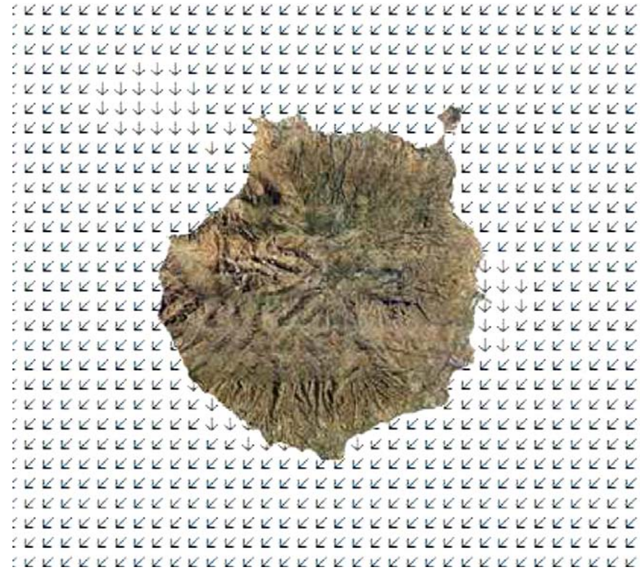


Fig. 8. Dominant wind direction – middle area.

As for number of operating hours, the Weibull distribution has been chosen as representative of this kind of parameter. This is a well known distribution, given by two coefficients, scale (C), and shape (k), that can be put in relationship with the mean value and standard deviation by means of the moments method. The Weibull distribution can be expressed using its probability distribution

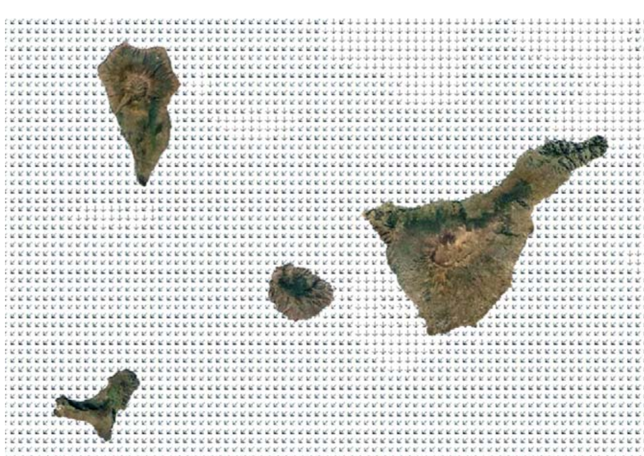


Fig. 7. Dominant wind direction – western area.

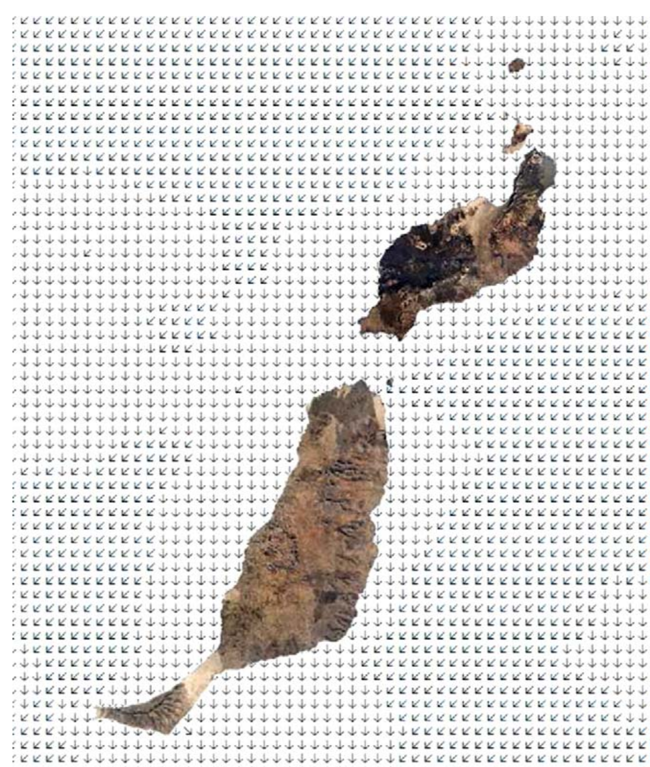


Fig. 9. Dominant wind direction – eastern area.

function according to (3).

$$P(x_i < x_0) = 1 - e^{-(x_0/C)^K} \quad (3)$$

where $P(x_i < x_0)$ denotes the probability that $x_i < x_0$.

The values of K and C can be calculated according to (4) and (5):

$$K = \left(\frac{S}{\bar{X}}\right)^{-1.086} \quad (4)$$

$$C = \bar{X} \cdot \left[\Gamma\left(1 + K^{-1}\right)\right]^{-1} \quad (5)$$

where Γ is the Gamma function of Legendre.

When trying to check the fitting level between the approximated function and the observed distribution, the following aspects can cause differences:

1. Fluctuations during the sampling process.
2. The observed distribution does not correspond to the law as was assumed.

In order to establish the fitting level, a Smirnov–Kolmogorov test [27] has been carried out, by defining a hypothesis $H_0 : F(x) = F_0(x)$, to compare both distributions. H_0 is rejected when there is a significant difference between both distributions. In mathematical terms, the test is defined by means of (6) and (7):

$$D_n = \max |S_n(x) - F_o(x)| \quad (6)$$

$$S_n(x) = \begin{cases} 0 & x < x_k \\ k/n & x_k \le x < x_{k+1} \\ 1 & x \ge x_n \end{cases} \quad (7)$$

The distribution of D_n is independent of the proposed model under H_0, with the result that it can be assessed exclusively as a function of the sample size. The error, α, can be established as a function of a critical region given by (8):

$$p\left(D_n > \frac{C}{\sqrt{n}}\right) = \alpha \quad (8)$$

Kolmogorov–Smirnov test is not used in all those cases where the observations are inherently quantitative due to the ambiguities that can appear when putting the observations in order.

Once the method and test that have been used for the calculation of the operating hour maps have been commented on, it becomes necessary to explain that two kinds of estimators have been defined: the first one by stretches (around, under and above the mean value); and a different, full type one. Several maps can been elaborated for these options, although they are not all included in this paper.

7.2.1. Estimation of operating hours around the mean value of the calculated speed

The number of hours during which a given generator will be working in an interval close to the mean speed is calculated on the mean value map. Such an interval is determined by upper and lower limits of 5% around the mean value.

Losses are estimated as 2% (due to non-operating hours for maintenance and the like), which, over 1 year, results in 175.2 h.

7.2.2. Estimation of operating hours under the calculated mean speed

The number of hours during which the generator will be operating under the calculated mean speed is estimated according to the mean speed map. The interval that is computed for the estimation begins in the cut-in value (that we are considering equal to 3 m/s), and goes up to the 95% of the mean speed at that point.

It is also assumed that global losses reach values of 4%, i.e., 350.4 h.

7.2.3. Estimation of operating hours above the calculated mean speed

The number of hours during which a given generator will operate above the mean speed is estimated. The interval is computed from 105% of the mean speed and 30 m/s.

A value of 4% is also considered for the losses.

By analyzing the previous maps, the conclusion can be that the total operating hours are in the interval of 1500–2000.

7.2.4. Estimation of operating hours grouped by the wind potential index

The operating hours valid for wind generation at nominal power are estimated taking into account the design at each domain. As the nominal power is very variable according to the manufacturer and features of each machine, an interval given by the most usual speeds has been used. When dealing with offshore wind turbines, these are 7, 8, 9, 10, 11 and 12 m/s.

The wind potential index (*WPI*) allows us to classify the different areas according to the number of equivalent operating hours (*eh*) per year valid for wind generation.

Four categories have been established:

- $WPI = 1 \rightarrow eh \le 2900$ h
- $WPI = 2 \rightarrow 2900\text{ h} < eh \le 3300$ h
- $WPI = 3 \rightarrow 3300\text{ h} < eh \le 3700$ h
- $WPI = 4 \rightarrow eh \ge 3700$ h

According to the previous map, it can be observed that almost 90% of the calculated domain results in *WPI* = 3. There are three areas with *WPI* = 4, one of them located to the northwest of La Gomera, a second one to the west of Gran Canaria and south of Tenerife and a third one to the east of Gran Canaria. The area with lowest value of *WPI* is to the southwest part of Tenerife, including a part of the coast of La Gomera.

As a summary, comparing data from the mean wind speed map and data from the operating hour estimation maps, the conclusion can be reached that the highest wind speeds (interval from 8 to 10 m/s) and the greatest number of operating hours can be reached in three areas: The eastern part of Gran Canaria, with an approximate surface of 135 km^2, the southeastern part of Tenerife and the western part of Gran Canaria, with a surface of approximately 200 km^2, and the northeastern part of La Gomera, with an equivalent surface of 100 km^2.

8. Data extrapolation

One of the most meaningful phenomena when exploiting wind energy is wind shear. Due to the friction of the air mass with the Earth surface, wind speed decreases from an undisturbed value at great height to a value of 0 at ground level. The Earth limit layer consists of a number of layers, each of them governed by a different set of flux parameters. However, the layer closest to the surface and the Ekmann layers are the most interesting for structure design [28]. The surface layer, from the ground to approximately 100 m height, is the region where the variation of the shear tension can be neglected, and this is the area where the wind turbines are located.

Hiester and Pennell have pointed out that only measurements taken at the height of the hub of a wind turbine will provide enough accuracy for a reliable calculation of the wind resource [29]. However, for preliminary estimations, it is possible to reduce the cost of taking measurements at great heights by using measurements taken at a reference height, and then extrapolating them.

Generally, a neutral atmosphere is considered, and a value of roughness, z_0, is estimated. Then, (9) is employed to estimate the mean wind speed at a height z, knowing the wind speed at a height h.

$$v(z) = v(h) \cdot \left[ln\left(\frac{z}{z_o}\right) / ln\left(\frac{h}{z_o}\right) \right] \tag{9}$$

(9) is a well known equation, frequently employed in energy analysis in Europe. For use in the offshore wind atlas of the Canary Islands, data are extrapolated to 4 typical hub heights (40, 60, 80 and 100 m). The results can be represented on several maps.

By means of an exhaustive analysis of all the maps obtained after the extrapolation at these different heights, we can accept that there is no great variation between the results calculated initially for 10 m and those from this extrapolation, due to the low level of roughness of the ocean.

9. Estimating offshore wind power generating capacity in the Canary Islands

As a general balance we have analyzed the offshore wind power that can be obtained in the Islands with wind turbine generator technology existing at present.

On the basis of the maps obtained for the mean value and the estimation of operating hours, the studied domain is classified according to the wind potential, from which the wind power capability in offshore locations has been calculated. The following hypotheses have also been considered:

- A very general estimate has been made for the marine areas located inside Spanish territorial waters.
- For this purpose, wind turbine generators between 1.5 and 5 MW have been employed.
- The wind turbine generator distribution on the terrain has been assumed on the basis of the dimensions of the machines employed during the study, and also the distribution of wind directions has been taken into account, for each area, according to data obtained from the Dominant Wind Direction Map given in Figs. 7–9.
- The results of power capacity are given according to the kind of foundation the generator has, because this has influence on the depth.
- Locations with $WPI < 3$ are not accepted. In all these marine domains there are areas that could be environmentally sensitivity and have been declared protected, these include natural areas, bird conservation areas, marine life areas, and so on. These areas have to be excluded from wind park installation.

In Table 1 results have been given of the total offshore wind power that could be installed for two kinds of wind turbine generators, i.e., type I (with a foundation fixed at the bottom of the sea), and type II (floating).

Table 1
Offshore wind power that can be installed with different types of wind turbine generators.

Island	Wind power (MW) I	Wind power (MW) II
La Palma	171	771
El Hierro	107	342
La Gomera	139	696
Tenerife	428	1414
Gran Canaria	332	1510
Fuerteventura	846	2592
Lanzarote	589	1660
Total	2612	8985

Table 2
Offshore wind energy that can be obtained with different types of wind turbine generators.

Island	Wind energy (GWh) I	Wind energy (GWh) II
La Palma	608.27	2742.57
El Hierro	380.62	1216.54
La Gomera	380.56	1905.55
Tenerife	1171.80	3871.33
Gran Canaria	1511.33	6873.83
Fuerteventura	1572.78	4817.50
Lanzarote	1170.50	3298.86
Total	6795.86	24526.18

It is also very important to understand that Table 1 shows wind power potential in offshore areas, but that we do not consider here electrical network capability for integrating such an amount of power, a task which is beyond the remit of this paper. A deeper analysis of such data allows us to think about the fact that, although the islands of Fuerteventura and Lanzarote present higher values of possible power to be installed, this does not mean that wind speeds are higher there.

Using previously described criteria we can venture to show what production by means of offshore wind parks would be. Assuming the described Weibull distribution for this task, in Table 2 we can see the results obtained, also for both kinds of wind generator.

A comparison between the 24,526 GWh of estimated offshore wind production and the trend in forecasted demand for the period 2008–2015 for the Islands, the conclusion is that offshore wind production would be able to cover the demand not only in 2015, but perhaps also until 2030. This would not be a real situation due to power system penetration limits and other factors.

10. Conclusions

In this paper, an offshore wind atlas for the Canary Islands is presented. Such an atlas is based on three combined models, by computing a wide data set. Three maps have been drawn up, one for Mean Wind Speed, one for Mean Wind Direction and one for Dominant Wind Direction. Studying them allows us to conclude that a great offshore wind power resource is available in the islands. The estimate of offshore wind power generating capability also indicates a high value.

Acknowledgement

This work has been partially funded by the company ZECSA, which is gratefully acknowledged by the authors.

References

[1] Economou A. Renewable energy resources and sustainable development in Mykonos (Greece). Renewable and Sustainable Energy Reviews 2010;14(5): 1496–501.
[2] Khalifa K. Mapa eólico del norte de Mauritania: aplicación a la generación de energía eléctrica. Ph.D. thesis. Universidad Las Palmas G.C.; 2000.
[3] Carracedo J. The Canary Islands: an example of structural control on the growth of large oceanic-island volcanoes. Journal of Volcanology and Geothermal Research 1994;60(3–4):225–41.
[4] Clift P. Geophysics of the Canary Islands: Results of Spain's Exclusive Economic Zone Program. Berlin: Springer; 2005, ISBN 1402033257.
[5] Navegador online del recurso eólico de Canarias. Instituto Tecnológico de Canarias 2009; 2009. http://hipocrates.itccanarias.org/recursoeolico/.
[6] Mapa y predicción eólica. Instituto Tecnológico de Canarias; 2006. http://www.renovae.org/index.php?option=com_docman&task=doc_download&gid=100&Itemid=44.
[7] Ramírez P. Modelado estadístico de las características del viento para su evaluación energética. Aplicación a las Islas Canarias. Ph.D. thesis. Universidad Las Palmas G.C.; 2006.

[8] Burton T, Sharpe D, Jenkins N, Bossanyi E. Wind energy handbook. John Wiley & Sons; 2002, ISBN 0-471-48997-2.
[9] Heard D. Analytical techniques for atmospheric measurement. Wiley-Blackwell; 2006, ISBN 1405123575.
[10] Lalas D. Modelling of atmospheric flow fields. World Scientific Pub Co Inc; 1996, ISBN 9810225091.
[11] Manwell J, McGowan J, Rogers A. Wind energy explained: theory, design and application. Chichester: John Wiley Sons Ltd; 2002, ISBN 0470846127.
[12] Soriano C, Jorba O, Baldasano JM. One-way nesting versus two-way nesting: does it really make a difference? Air pollution modeling and its application XV.. New York: Springer, US; 2002, ISBN 9780306472947.
[13] Astrup C, Nielsen P, Hasager P. QuikSCAT and SSM/I ocean surface winds for wind energy. In: Geoscience and Remote Sensing Symposium, 2007. IGARSS 2007; 2007.p. 3507–12.
[14] Chang P. Ocean Surface Winds Derived from the SeaWinds Scatterometer; 2009. http://manati.orbit.nesdis.noaa.gov/quikscat/.
[15] USDO. Passive microwave observing from environmental satellites: NOAA technical report NESDIS 35 (US Department of Commerce, Washington, 1987. 292+iii pp), Space Policy 1988;4(2):176–6. http://www.sciencedirect.com/science/article/B6V52-47X7BG3-GC/2/6e9b456fbe71751d580b26cccfcb1cd5.
[16] Cats GWL. The Hirlam project [meteorology]. Computational Science Engineering IEEE 1996;3(4):4–7.
[17] Marti I, Nielsen TS, Madsen H, Navarro J, Barquero C. Prediction models in complex terrain. In: European Wind Energy Conference 2001. Copenhagen; vol. 1. Sylvensteinstr. 2, D-81369 Munchen/Piazza Savonarola, 10, I-50132 FLorence: WIP-Renewable Energies/ETA; 2001, p. 875–8. http://www2.imm.dtu.dk/pubdb/p.php?682.
[18] AEMET meteosea; 2009. http://www.aemet.es/es/eltiempo/prediccion/maritima.
[19] Grell G, Dudhia J, Stanffer D. A description of the fifth-generation Penn State/NCAR mesoscale model (MM5). Tech. Rep.; NCAR/TN 3981 STR; 1995. NCAR Technical Note.
[20] Instituto Tecnológico y de Energías Renovables; 2009. http://www.iter.es/.
[21] Red Iberica de Usuarios de MM5; 2009. http://redibericamm5.uib.es/.
[22] Ohring G. NOAA Satellite programs in support of a global change program. Advances in Space Research 1989;9(7):295–9. http://www.sciencedirect.com/science/article/B6V3S-4725PVW-1D/2/4637890a1c6d6ea4a7ccb9146c390392..
[23] Ahn JSJMG. The application of sea level pressure and vorticity fields derived from the university of Washington planetary boundary layer model in the NOAA ocean prediction center; 2006. p. 1–6.
[24] Michalakes J, Hacker J, Loft R, McCracken MO, Snavely A, Wright NJ, et al. WRF nature run. In: SC'07: Proceedings of the 2007 ACM/IEEE conference on Supercomputing. New York, NY, USA: ACM; 2007. p. 1–6. ISBN 978-1-59593-764-3.
[25] Corotis RB, Sigl AB, Klein J. Probability models of wind velocity magnitude and persistence. Solar Energy 1978;20(6):483–93. http://www.sciencedirect.com/science/article/B6V50-497SRDJ-JH/2/d8e72142e0ff987aaf2a7b8d3cb7cd26..
[26] Anderson OD. Time series analysis: forecasting and control (revised edition) by George E.P. Box and Gwilym M. Jenkins. 575 pages, diagrams, 6×9 in., Holden-Day, San Francisco, 1976. Journal of the Franklin Institute 1980;310(2):144. http://www.sciencedirect.com/science/article/B6V04-45D9SM9-G/2/11b18c51489e5e7aeea2c7de79ff4247..
[27] Lilliefors HW. On the Kolmogorov–Smirnov test for normality with mean and variance unknown. Journal of the American Statistical Association 1967;62(318):399–402. http://www.jstor.org/stable/2283970.
[28] Freris L. Wind energy conversion systems. Englewood Cliffs: Prentice Hall; 1990, ISBN 0139605274.
[29] Hiester B. The siting handbook for large wind energy systems. Rockville Centre: Windbooks; 1983, ISBN 0880160047.